

OPTICAL AND ELECTRICAL PROPERTIES OF CHEMICAL BATH DEPOSITED COBALT SELENIDE THIN FILM

R. A. CHIKWENZE^{a*}, J. I. UBA^b, J. U. ARIKPO^a

^a*Department of Physics, Geophysics and Geology, Federal University, Ndufu-Alike, Ikwo, Nigeria*

^b*Department of Physics, Nwafor Orizu College of Education. P.M.B. 1734, Onitsha, Anambra, Nigeria*

This contribution presents optical and electric properties of Cobalt Selenide thin films whose bandgaps were altered. The CoSe samples were fabricated in chemical bath with polyvinyl alcohol (PVA) as matrix agent to modify the crystallite size so as to enhance the bandgaps and annealed at 100 – 250 K. Optical studies placed the bandgaps at 4.25 – 4.30 eV. About the same magnitude were found from electric conductivity test. Static dielectric constant of 1.2 was found for all samples irrespective of annealing. The samples exhibited high conductivity with increasing temperature at 303 – 373 K. However, with respect to annealing temperature, the conductivity decreased due to increased electron-phonon interaction, and indicated that water of crystallization attenuated lattice waves. The achieved wide bandgaps place CoSe fabricated with the presented method as a good material for power electronics devices.

(Received August 17, 2016; Accepted June 2, 2017)

Keyword: CoSe, Bandgap, Conductivity

1. Introduction

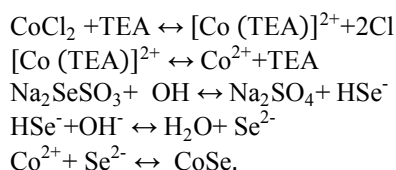
Many physical and chemical techniques exist for deposition of selenide compound thin films [1-4]. In recent times, chemical bath deposition (CBD) also known as solution growth or precipitation method, attracts much interest for the deposition of metal chalcogenides because it is relatively less expensive, convenient and simple and results in high quality, pin-hole free deposits and affords large area deposition [5-7]. A large range of binary and ternary alloy semiconductors from groups II – VI, V – VI, and III – VI has been synthesized using the CBD. The fabrication of binary metal chalcogenide of groups II-VI semiconductors in Nano crystalline form has been a rapidly growing area of research due to their important non-linear optical properties, luminescent properties, quantum size effect and other physical and chemical properties. The group A^{II}B^{IV} compounds have been found interesting for technical application because of their wide range of chemical, structural, electrical and optical properties [8]. CoSe is among the II-VI semiconductors with direct band gap. The structural, optical, chemical properties and mechanical stability makes it a semiconductor suited for microelectronics applications. Recent studies show that its bandgap varies with method of preparation. A chemical bath deposited sample had 0.4 eV bandgap [5], while a sample electrodeposited from acid bath exhibited 1.53 eV bandgap [9].

On the basis that materials properties could be influenced by changing the crystallite size through fabrication method and prevalent conditions, and Polyvinyl alcohol (PVA) is one means of modifying these sizes [10]; we have studied CoSe films deposited by CBD with PVA as growth matrix. The present contribution focuses on the optical properties and electric conductivity.

*Corresponding author: racychikwe@gmail.com

2. Materials and Methods

The deposition baths used were prepared with PVA as the growth matrix. The PVA solution was prepared by adding 900ml of distilled water to 1.8g of solid PVA $(-C_2H_4O)_n$ (where $n = 1700$) and stirred with a magnetic stirrer at 363K for 1 hour. The temperature of the resulting homogenous solution was allowed to drop to 298K. To make the deposition bath, 40ml of the PVA solution was added to an alkaline mixture of 5ml of 1M $CoCl_2$, 10ml of TEA and 5ml of 1M Na_2SeSO_3 . The bath was stirred and heated to 333K. The CoSe films were grown by dipping well cleaned glass substrates into the bath. The substrates were vertically hung using synthetic cover. The deposition reaction is summarized as follows:



The loaded substrates were taken out of the beaker after 1 hour, rinsed with distilled water and allowed to dry. Four of the five samples were annealed in a thermostatic blast oven for 1 hour at different temperatures in the range 373-673K at 50 K interval and labelled.

Energy dispersive X-ray (EDX) was used to ascertain the composition of the films and the grain sizes were studied via X-ray diffraction (XRD). The XRD was recorded using MD-10 mini diffractometer of CuK α wave length 1.5408Å. The XRD diffractograph of intensity versus 2θ , values were generated and displayed. Phase identification was then made from an analysis of intensity of peaks versus 2θ , using ICDD data. The average crystalline size of the films was then calculated from the recorded XRD pattern using Scherrer formula:

$$D = \frac{0.89\lambda}{\beta \cdot \cos(\theta)}$$

where D is the average crystallite size, λ the wavelength of incident X-ray, β the full width of half maximum (FWHM) of X-ray diffraction and θ is the Bragg's angle.

The electrical and optical properties of the grown and annealed films were probed with four-point-probe and UNICO-UV-2102P spectrophotometer respectively. The optical studies were done in the wavelength range of 275 – 1100 nm. The conductivity test was carried out from 303 – 373 K.

3. Results and Discussions

3.1 Compositional and grain size study

Analyses of a sample deposited at 0.25M concentration and annealed at 150K are given herein. Table I shows the elemental apparent concentration, weight % and atomic % of the substrate and the deposit generated by the EDX.

Table I: EDX analysis of substrate and CoSe thin film annealed at 150K

Element	Apparent Concentration	Intensity Corr'n	Weight %	Weight % Sigma	Atomic %
O K	59.27	0.7237	43.17	0.97	50.98
Na K	5.11	0.7328	3.68	0.23	3.02
Al K	1.00	0.6623	0.80	0.13	0.62
Si K	35.42	0.8672	21.54	0.50	14.49
Se K	2.74	0.7998	1.80	0.15	1.06
Ca K	7.79	0.9672	4.25	0.19	2.00
Co K	13.57	0.8059	8.88	0.42	2.85

From Table I, apart from O, Si, Al, Ca, and Na which are confirmed elemental compositions of the substrates by Rutherford Back Scattering (RBS) [4], the other elements present are Co and Se. This confirms that the deposited film is CoSe thin film. The corresponding XRD diffractograph is illustrated in Fig. 1. The mean crystallite size was estimated as 30.6nm.

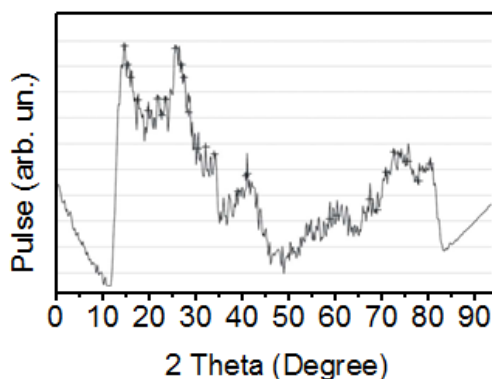


Fig. 1: XRD Diffractograph for CoSe thin film deposited at 0.25M concentration and annealed at 150K

3.2 Optical study

The optical characteristics of the samples are qualitatively the same over 275 – 1100 nm. The optical bandgap is deduced from the absorption coefficient as a function of photon energy. An instance is Fig. 2, for as-grown sample. As shown in Table II, CoSe thin films prepared with the present method have wide bandgaps that are considerably more than that of Liu et al [9] and ten times larger than that of CBD sample of Pramanik [11] reported in [5]. We attribute the difference from the latter to PVA and absence of hydrazine hydrate in our bath. Furthermore, there is no significant effect of annealing on the bandgap. However, annealing clearly influenced the structural morphology of the films as denoted by the respective Urbach energies (the reciprocal of the gradient of natural log of absorption coefficient as function photon energy).

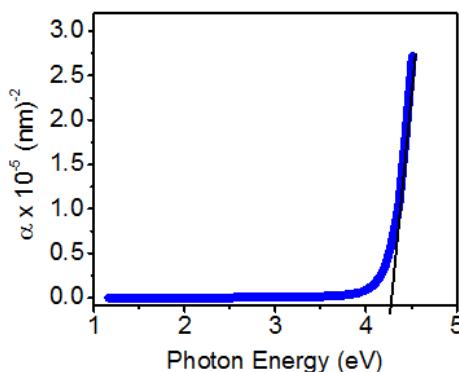


Fig. 2: Square of absorption coefficient for as grown sample.

Table II: Properties of chemical bath deposited CoSe in PVA matrix.

PROPERTY	AS GROWN	100°C ANNEALED	150°C ANNEALED	200°C ANNEALED	250°C ANNEALED
Bandgap (optical), eV	4.30	4.25	4.28	4.31	4.30
Bandgap (Elec.), eV	4.33	4.30	4.30	4.38	4.35
Urbach energy, eV	0.840	0.845	0.847	0.847	0.912
$\epsilon(0)$	1.20	1.20	1.20	1.20	1.20

Analyses of the real dielectric constants revealed that these do not follow the usual trend $\varepsilon(\omega) = 1 - \omega_p^2/\omega^2$ [12], where ω is angular frequency of radiation, $\omega_p^2 (=4\pi Ne^2/m_{op})$ the electron plasma frequency with N number of carriers and m_{op} , the optical mass of electron. Fig. 3 shows typical dispersion curve. This deviation implies the existence of variable relaxation time, τ , optical mass and electron plasma frequency over the range of wavelengths used in this study. The effect is exhibited in the transmittance and reflectance (Fig. 4). In Fig. 4, CoSe shows considerable reflectance in the interval 285 – 600nm only. Below and above this range, the reflectance is essentially zero, making the CoSe transparent to the corresponding wavelengths with ω_p much less than ω [13]. It should be noted that if $\varepsilon(\omega) = 1 - \omega_p^2/\omega^2$ were valid for the involved material, the reflectance would have been positive and non-zero across the wavelength range.

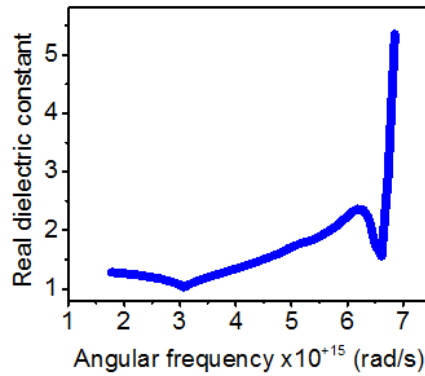


Fig. 3: Real dielectric constant as function of angular frequency of radiation for As-grown sample.

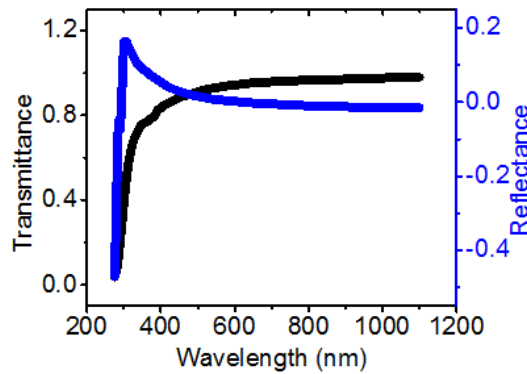


Fig. 4: Transmittance and reflectance curves for as-grown sample.

In addition, the dispersion curves of the samples rather than a smooth curve [13], spot two minima as illustrated in Fig. 3 for as-grown sample. The two anomalies underscore transitions in the reflectance. From 275 – 285 nm, the reflectance is negative (see Fig. 4), but increasingly positive from 285 nm. The 285nm marks the minimum in the dielectric constant in the region of high angular frequency and high photon energy. The reflectance falls to zero at 610 nm, that marks the second minimum in the dielectric constant in the region of low angular frequency and photon energy. Beyond the 610nm, the reflectance is increasingly negative up to 1100 nm. It is possible that the minima are due to interband transitions. If we take as-grown sample for instance, the bandgap, 4.3eV corresponds to a wavelength of 288nm, which is in the neighborhood of the minimum point (285 nm) of dielectric constant at high angular frequency (high photon energy) in Fig. 3. Thus, the minimum at low angular frequency (low photon energy) may stem from another transition; possibly an indirect transition. However, this aspect is not yet fully investigated. The

vertical intercepts of the dispersion curves give the static dielectric constant $\epsilon(0) = 1.2$ for all samples independent of heat treatment.

3.3 Electrical study

The samples' conductivities were measured from 303 – 373 K at 5K interval with four-point probe. They exhibited exponential characteristics of the form $\sigma = A \exp(-\frac{E_g}{k_B T})$ [13] that allowed determination of bandgaps from regression analyses. Fig. 5, is an instance of the measurement for as-grown film and samples annealed at 200°C and 250°C. The bandgaps thus deduced, are within the same order of magnitudes as those of optical studies and listed in Table II. There is a reduction of conductivity across the samples as evidenced in Fig. 5. We rule out structural imperfection as contributing factor to this reduction because annealing affords increasingly better structural morphology as indicated by the Urbach energy in Table II, which should encourage increase in conductivity with annealing. In light of this, we consider attenuation of phonons as the primary cause. This is because the sample annealed at 250K had the least conductivity at 373K and since annealing removes water of crystallization, electron-phonon interaction increases as sample is dehydrated. This implies that water of crystallization attenuates lattice waves.

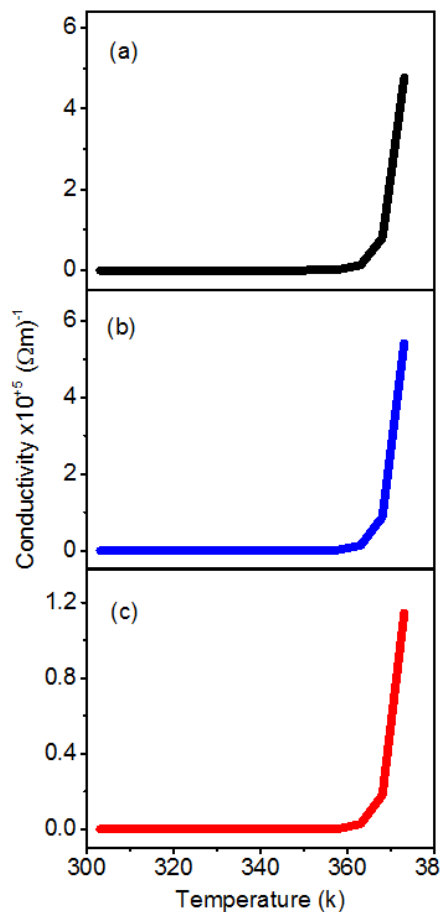


Fig. 5: Electric conductivities of samples. (a) as-grown. (b) 200°C annealed. (c) 250°C annealed. Conductivity decreases with annealing

4. Conclusion

The presented method of fabrication resulted to wide bandgap CoSe thin films that exhibited high conductivity at elevated temperature. Not only has this demonstrated the possibility

of controlling the bandgap of CoSe with PVA but also influenced the optical behavior of the material. From the latter, it is seen that lights in the visible range from 600nm can moderate the plasma frequency. Due to the wide bandgap, the CoSe as fabricated herein holds good promise in power electronics devices.

References

- [1] K.R. Murali, K. Sivaramamoothy, B.S. Asath, M. Kottisamy, *Chalcogenide Letters* **5**(11), 248 (2008).
- [2] N. C. Sharma, R.C. Kainthla, D.K. Pandya, K.L. Chopra, *Thin Solid Films* **60**, 55 (1979).
- [3] E. Vigil, L. Saadoun, J.A. Ayllon, X. Domenech, I. Zumeta, R. Rodriguez-Clemente., *Thin Solid Films* **365**, 12 (2000).
- [4] R.A. Chikwenze, M.N. Nnabuchi, *Chalcogenide Lett.* **7**(5), 401 (2010).
- [5] R.S. Mane, C.D. Lokhande, *Materials Chemistry and Physics* **65**, 1 (2000).
- [6] F.I. Ezema, S.C. Ezeagwu, A.B.C. Ekwealor, P.U. Asogwa, *Journal of Ovonic Research* **5**(5), 49 (2009).
- [7] P.U. Asogwa, S.C. Ezugwu, F.I. Ezema. *Superficies y Vacio.* **23**(1), 12 (2010)
- [8] K.D. Patel, R.K. Shah, D.I. Malhija, V.M. Pathak, R. Srivastava, *Journal of Ovonic Research* **A**(6), 129 (2008).
- [9] F. Liu, B. Wang, Y. Lai, J. Li, Z. Zhang, Y. Liu, *J. Electrochem. Soc.* **157**(10), 523 (2010).
- [10] R.A. Chikwenze, M.N. Nnabuchi, *Optoelectron. Adv. Mat.* **12**(12), 2363 (2011).
- [11] P. Pramanik, S. Bhattacharya, P.K. Basu, *Thin Solid Films* **149**, L81 (1987).
- [12] Animalu A.O.E., *Intermediate quantum Theory of Crystalline Solids*, Prentice-Hall, New Jersey, 1977.
- [13] Ziman J.M., *Principles of The Theory of Solids*, 2nd ed., Cambridge University Press, (1972).